

A NON-NEWTONIAN FINITE ELEMENT ANALYSIS OF BLOOD FLOW IN THE ARTERIAL NETWORKS

Y. Dabiri¹, N. Fatouraei^{*2} and H. Katoozian³

Biological Fluid Dynamics Research Laboratory, Biomedical Engineering Faculty, Amir Kabir University of Technology (Tehran Polytechnic), Tehran, Iran 15914

¹Y_dabiri4@Yahoo.com, ²Nasser@aut.ac.ir, and ³Katoozian@engineer.com

Abstract: To examine the effect of blood non-Newtonian models, arterial stenosis and arterial taper on pressure and flow waves is the goal of this study.

The finite element technique is used to solve one-dimensional blood flow equations in an arterial network.

The pattern of calculated propagating waves agrees with experimental reports in the literature.

Simulations done by different models of blood showed the Newtonian and Casson models produce similar results but the Power Law model underestimates shear force. Considering this fact that in large arteries blood behaves as a Newtonian fluid, the Casson model gives more accurate results than the Power Law model.

Examining the compliance of capillary beds showed it has a great role in reducing distal wave reflections, relatively.

Simulation of stenosis showed that it reduces blood pressure and flow in its downstream locations and a more severe stenosis produces more reduction.

The analysis of area taper showed that the effect of taper on the results depends on the difference between areas in tapered and no tapered arteries and that the taper does not have a certain effect on the results.

Introduction

The physiological importance of blood flow in the arterial system has motivated a lot of researchers to simulate it. The complications involved in this system have made the researchers impose simplifying assumptions in their models. The most important assumption is the one-dimensionality of the blood flow. Nevertheless, the remained complexities have produced other computational problems.

Using electrical circuits to model arteries has extensively been used to overcome these complexities. But using the computational fluid dynamics (CFD) is the more appropriate approach to handle the three dimensionality complexities. The method of characteristics [1], the finite difference method [2] and the finite element method [3 and 4] are examples of the CFD based modeling.

In this research, with the one-dimensional assumption of blood flow, the finite element method has been used to solve mathematical equations. The novelty

of this work is on using this technique in a different way than previous studies. In addition, modeling blood as a non-Newtonian fluid and the assessment of the role played by arterial taper are other differences between this study and the previous ones.

Materials and Methods

As mentioned in the previous section, the essential assumption is the one-dimensionality of blood flow. Also, it is assumed that arteries are elastic tapered tubes and blood flow is laminar.

The one-dimensionality assumption is not acceptable in locations like arterial branches, arterial stenoses and stepwise changes of the arterial area where blood flow encounters sudden discontinuities. Therefore, governing equations in these locations are not the same as those in a healthy straight artery.

Based on above explanations physical modeling includes five different cases.

A healthy Artery. The governing equations in this case are the one dimensional continuity and momentum equations which are, respectively:

$$\frac{\partial A}{\partial t} + \frac{\partial(VA)}{\partial x} = 0, \quad (1)$$

$$\frac{\partial P}{\partial x} + \rho \frac{\partial V}{\partial t} + \rho V \frac{\partial V}{\partial x} + \frac{f_\tau}{A} = 0. \quad (2)$$

where P , V and ρ are blood pressure, velocity and density respectively, A is arterial area, f_τ is the shear force per unit length at the arterial wall and finally t and x are time and space dimension respectively. The relation between A and P is as follows:

$$A(P, x) = A(P_0, x) [1 + C_0(P - P_0) + C_1(P - P_0)^2]. \quad (3)$$

where P_0 is initial pressure, C_0 and C_1 , are the arterial compliance coefficients, which are obtained from other equations of state by performing a Taylor series expansion. In this study the following equation of state, Streeter model, has been used [5]:

*Corresponding author

$$A(P, x) = A(P_0, x) \left[1 - \frac{\left(\frac{d_0}{h_0} \right) (P - P_0)}{E} \right]^{-1} \quad (4)$$

where d_0 , h_0 and E are arterial diameter, thickness and Young's modulus respectively. For this model we have:

$$C_0 = \frac{1}{Eh_0} \sqrt{\frac{4A_0}{\pi}}, C_1 = \frac{4A_0}{\pi E^2 h_0^2} \quad (5)$$

The relation between f_τ and V is obtained by solving the steady state momentum equation. The final relation depends on the model used for blood. In this study the Power Law and Casson models have been used in addition to the Newtonian one. All of these models can be written in the following form:

$$\tau = \mu \dot{\gamma} \quad (6)$$

where τ is shear stress; $\dot{\gamma}$ is shear rate and μ is effective viscosity. These models and their corresponding f_τ are given in Table 1. For more details of these models see [6].

Arterial Branch. The governing equations in a branch conserve the mass passing through it and cause the pressure to be constant at the outlet of parent artery and the inlet of daughter arteries:

$$A_p V_p = \sum_{i=1}^n (A_d V_d)_i \quad (7)$$

$$P_p = (P_d)_i \quad (8)$$

where indexes P and d refer to parent and daughter arteries, A , V and P are respectively arterial area, blood velocity and pressure.

Considering the fact that the dynamic pressure of blood is very small in comparison to its transient pressure, the second equation is acceptable. This assumption has been used in previous studies [e.g. 1, 2, 3 and 4].

Arterial Area Discontinuity. As mentioned previously, it is assumed that arteries are elastic tapered tubes. In order to model taper, the arterial area is reduced in a stepwise manner. In a location where two arteries with different areas connect, the mean velocity is not continuous. Therefore, we do not connect these arteries directly. Instead, they are connected in a manner like an arterial branch. In other words, the governing equations in their connection are so that the mass is conserved and blood pressure does not change.

Arterial Stenosis. One of the most common diseases of cardiovascular system is arterial stenosis. Therefore we have included it in our modeling. The corresponding governing equations, taken from [7], are:

$$\frac{\partial V}{\partial x} = 0, \quad (9)$$

$$\frac{\Delta P}{\rho L} - K_v \frac{\mu}{DL\rho} V - \left(\frac{K_t}{2L} \right) \left[\frac{A_0}{A_1} - 1 \right]^2 V|V| - K_u \frac{\partial V}{\partial t} = 0. \quad (10)$$

where L is the length of the stenosis, ΔP is pressure drop across the stenosis, D & A_0 are diameter and area of the unobstructed artery and A_1 is the area of the stenosis. K_t , K_u and K_v are constants dependent on geometry of the stenosis. In this study they are, respectively: 1.5, 1.2 and

$$K_v = 32 \left[\frac{0.83L + 1.64D_1}{D} \right] \left(\frac{A_0}{A_1} \right)^2$$

where D_1 is the diameter of the stenosis.

Peripheral Beds. The peripheral arteriole and capillary beds at the ends of arteries have been modelled in two ways: a) as an electrical circuit known as developed Windkessel model. The relation between blood pressure and velocity in the inlet of this model (outlet of upstream artery) is:

$$C_T \frac{dP}{dt} - R_1 C_T \frac{d(VA)}{dt} + \frac{P}{R_2} - \left(1 + \frac{R_1}{R_2} \right) (VA) = 0. \quad (11)$$

where C_T , R_1 and R_2 are parameters of corresponding electrical circuit, V , P and A are blood velocity, pressure and arterial area at the outlet of upstream artery; b) an electrical circuit known as pure resistance model, that is:

$$P = RVA. \quad (12)$$

where R is the resistance of electrical circuit, V , P and A are the same as in the developed Windkessel model.

With physical equations in hand, FEM has been used to solve them in an arterial network. The FEM modeling is shortly explained.

Based on five physical cases mentioned above, three elements have been used. These elements are artery element, branch element and stenosis element that are respectively for a healthy artery, an arterial branch (or sudden area reduction) and an arterial stenosis. The fifth case, peripheral beds, are the boundary conditions.

Artery Element. The Galerkin finite element method has been used to discretize equations (1) and (2), as follows:

$$\int N^T \left\{ \frac{\partial A}{\partial t} + \frac{\partial(VA)}{\partial x} \right\} dx = 0, \quad (13)$$

$$\int N^T \left\{ \frac{\partial P}{\partial x} + \rho \frac{\partial V}{\partial t} + \rho V \frac{\partial V}{\partial x} + \frac{f_\tau}{A} \right\} dx = 0. \quad (14)$$

Table 1: Blood Models

Model	Effective viscosity given in P (1 P = 0.1 Pa.s)	Shear force per unit length
Newtonian	$\mu = 0.0345$	$f_\tau = 8\pi\mu V$
Power Law	$\mu = \mu_0(\dot{\gamma})^{n-1}$ with $\mu_0 = 0.035$ and $n = 0.6$	$f_\tau = 2\pi\mu \frac{3n+1}{n} V$
Casson	$\mu = \left[(\eta^2 J_2)^{\frac{1}{4}} + 2^{-\frac{1}{2}} \tau_y^{\frac{1}{2}} \right]^2 J_2^{-\frac{1}{2}}$ where $ \dot{\gamma} = 2\sqrt{J_2}$, $\tau_y = 0.1(0.625H)^3$ and $\eta = \eta_0(1-H)^{-2.5}$ with $\eta_0 = 0.012$ P and $H = 0.37$	$f_\tau = \mu \frac{2\pi \left(2 + \frac{2r_p}{R} - 4\sqrt{\frac{r_p}{R}} \right) V}{\frac{1}{2} \left(1 - \frac{16}{7} \left(\frac{r_p}{R} \right)^{\frac{1}{2}} + \frac{4}{3} \left(\frac{r_p}{R} \right) - \frac{1}{21} \left(\frac{r_p}{R} \right)^4 \right)}$

In equations (13) and (14), N^T , the transposed shape function vector, is linear.

Branch Element. The governing equations in a branch are matrix form of equations (7) and (8).

Stenosis Element. Like branch element, the equations in a stenosis element are matrix forms of its governing physical equations, (9) and (10).

After assemblage step, the implicit method has been used for time dimension discretization. Then the boundary conditions are imposed. The inlet boundary condition is inlet pressure or velocity wave and outlet boundary conditions are based on equation (11) or (12). The resultant nonlinear system of equations is solved by the direct iteration and the Gauss elimination methods. All of the computational manipulations are done by C++ programming language.

Results

To assess the accuracy of computational procedures a model of foot arterial network, shown in Figure 1, was analysed.

It is assumed the hypogastric and profunda arteries have uniform cross sectional areas. The function of other arteries taper is [2]:

$$\begin{aligned} A(p_0, x) &= 0.505 \exp(-0.192\sqrt{x}) \quad 0 \leq x \leq 13 \\ A(p_0, x) &= 0.327 \exp(-0.0206x) \quad 13 \leq x \leq 60 \end{aligned} \quad (15)$$

Where, the distance from inlet, x is in cm and area, A , in cm^2 . As mentioned previously, the taper is modelled by stepwise reduction of arterial area.

The other data used for this model, including mechanical properties and distal peripheral beds parameters, are taken from [1 and 3].

The pressure wave at iliac bifurcation, taken from [3], is the inlet boundary condition and the developed Windkessel model has been used for peripheral beds (outlet boundary conditions).

The length of each element is maximally 2 cm and the time step is 0.004 s. With these specifications the solution time on a computer model Celeron Intel (R) CPU 1.70 GHz, 256 Mb RAM was approximately 15 minutes.

ILIAC BIFURCATION

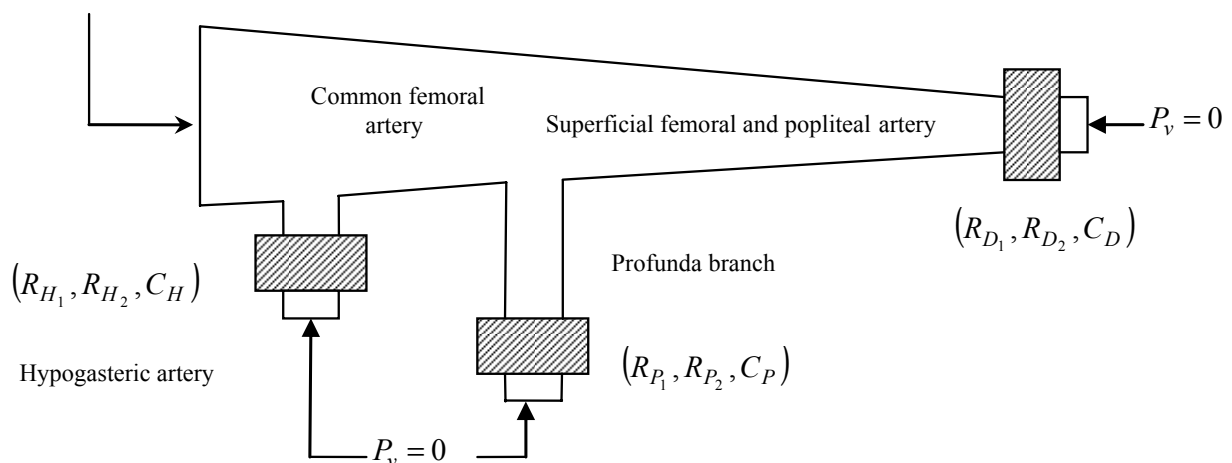


Figure 1: A schematic of foot arteries. P_v is the venous pressure and R_1 , R_2 and C are parameters of equation (11).

The pressure and flow waves at inlet, right after first branch, right after second branch and at distal popliteal artery are shown in figures 2 and 3, respectively. As the waves propagate away from inlet, the pressure wave amplifies, the mean pressure reduces and the flow wave peak and mean values decrease. These qualitative characteristics have been reported experimentally [8] and numerically [2 and 3].

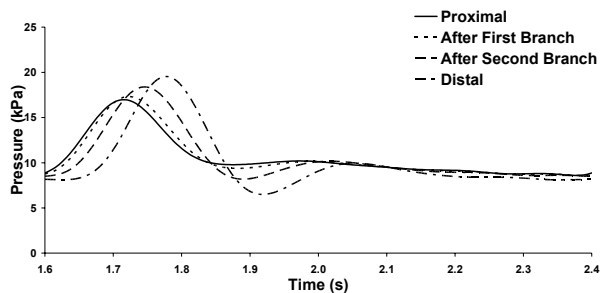


Figure 2: The pressure waves at four locations of Fig. 1

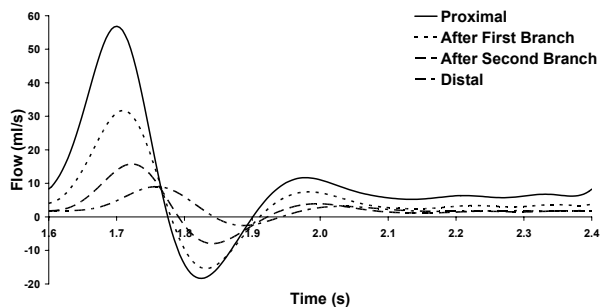


Figure 3: The flow waves at four locations of Fig. 1.

To compare different models of blood, in figure 4, pressure wave at distal popliteal is shown for each model and also for no shear force case. As this figure shows the Casson model produces results similar to Newtonian one but the Power Law model underestimates the shear force. In general, the Casson model produces more accurate results than Power Law model because it confirms the known fact that in large arteries blood can be considered as a Newtonian fluid. As we decrease the inlet pressure wave, the results of Power Law model get closer to results of Newtonian and Casson models. Therefore, it can be concluded that our arterial network parameters, especially arterial areas, are the main reasons of difference between different models of blood.

To compare equations (11) and (12) proposed for peripheral beds, the model was analysed when the equation (12) is imposed at the outlets.

Figure 5 shows the pressure wave at distal popliteal for each of equations (11) and (12). As this figure shows the pure resistance model produces stronger reflection than developed Windkessel model. This result agrees with that reported in [9]. The reason is the compliance included in the latter model. Considering the compliance nature of peripheral beds,

the developed Windkessel model produces more accurate results than pure resistance one. But evaluating the parameters of this model so they result the reflections seen in the real system, is in question. Nevertheless from figure 5 it is seen that the compliance of capillary beds has a noticeable effect on results.

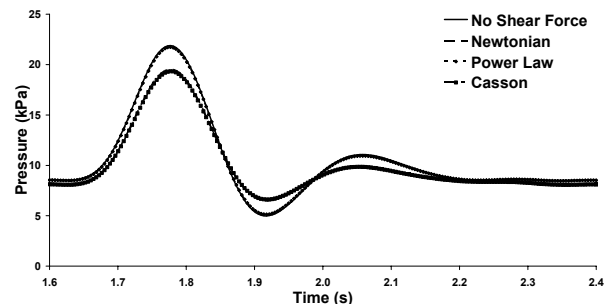


Figure 4: Distal pressure wave for different blood models and no shear case.

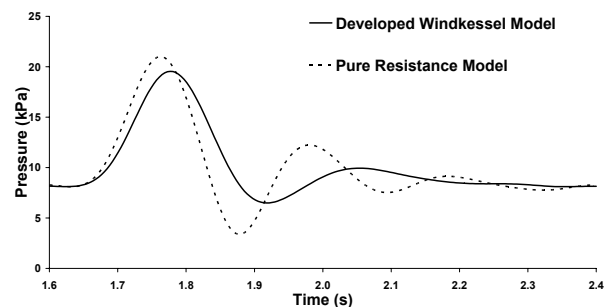


Figure 5: Distal pressure resulted from two models of peripheral beds.

In order to investigate the effect of arterial stenosis on results, a stenosis was placed in the main artery 40 cm from the iliac bifurcation and its severity was changed from 0 to 90 percent obstruction. The pressure and flow waves at distal popliteal are shown for different severities of stenosis in figures 6 and 7.

As can be seen in these figures, stenosis causes reduction of pressure and flow after it and the more severe the stenosis is, the more reduction is seen. These results, usable in detection of stenoses, have been reported in previous studies [1 and 3].

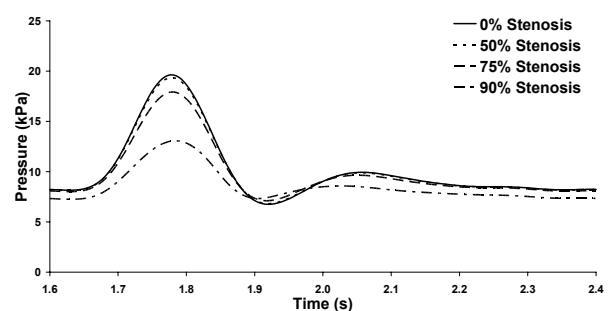


Figure 6: Pressure wave at distal popliteal for 0, 50, 75 and 90% stenoses.

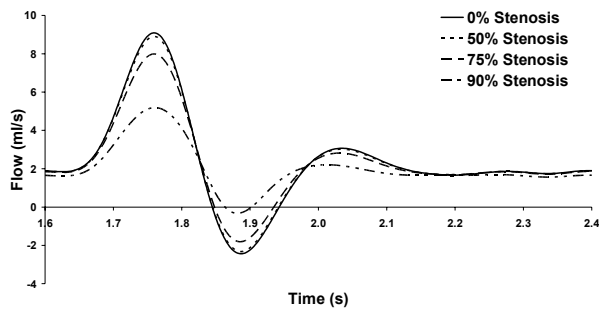


Figure 7: Flow wave at distal popliteal for 0, 50, 75 and 90% stenoses.

Arteriosclerosis. In arteriosclerosis the arteries become stiffer. To simulate this disease the Young's modulus of popliteal artery (after second branch) was increased by 25%. The pressure wave at distal popliteal for this case and healthy model are shown in figure 8. As this figure shows, arteriosclerosis reduces pressure wave amplification. This result agrees with experimental reports [10].

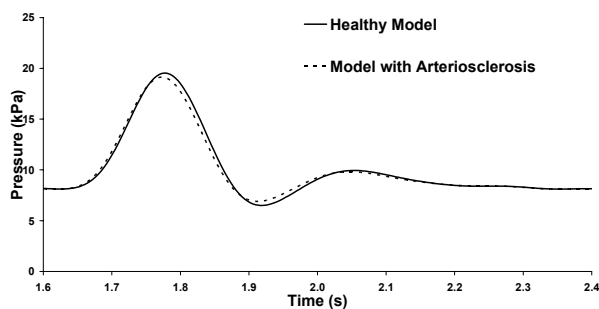


Figure 8: Pressure wave at distal popliteal for healthy and with arteriosclerosis models.

Arterial Taper. The main goal of this paper is analysing the effect of arterial taper on results.

To investigate the effect of taper on results the convective and viscous terms in momentum equation were ignored and the branches of main artery in figure 1 were closed. The resultant straight tube was analysed. Its distal pressure wave is shown in figure 9 for four cases. a) when it is tapered just as was mentioned for figure 1; b) when it has 0.196 cm² area; (c) when it has 0.505 cm² area (proximal area in tapered case) and (d) when it has 0.095 cm² area (distal area in tapered case).

The comparison between cases (a) and (b) shows in tapered artery, pressure wave is amplified and proximally shifted. Reference [2] has done a comparison between cases (a) and (b) like us. The changes in pressure wave with arterial taper, reported in this reference, agree completely with our results.

When cases (a) and (c) are compared it is seen that in a tapered artery, pressure wave has lower peak and is proximally shifted. Considering equations (3) and (5), the effect of arterial taper is similar to arteriosclerosis because both of them reduce C_0 and C_1 . Therefore,

like arteriosclerosis, the arterial taper reduces pressure wave amplification and shifts it proximally.

Finally, when we compare cases (a) and (d), it is seen that in tapered artery, pressure wave is more amplified and proximally shifted. In this case the tapered artery has larger overall area than the no tapered one. Therefore, the results of their comparison can be interpreted similar to cases (a) and (b).

In general it is concluded that the effect of arterial taper depends on tapered and no tapered arteries and the taper does not have a certain effect on pressure and flow waves.

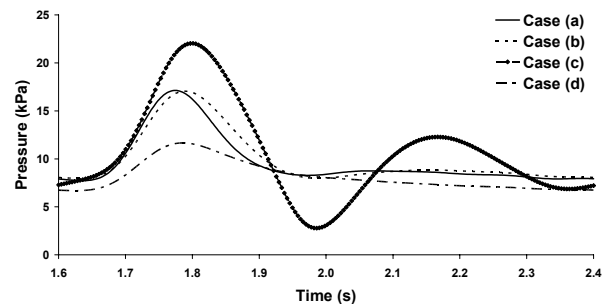


Figure 9: Distal pressure wave for different cases: when artery is tapered and when it has 0.196, 0.505 and 0.095 cm² uniform area, respectively.

Discussion

The results obtained for femoral artery show good agreement with experimental reports and the previous studies, qualitatively. In order to make our computer simulation useable in medicine, it is necessary to compare its results with experimental recorded pressure and flow waves. Unfortunately, we could not find a reference that gives us all of the input data required for computer simulation namely, the parameters of peripheral beds, mechanical properties of arteries, length and areas of arteries and pressure and/or flow waves in some points of an arterial network. Nevertheless, we ourselves are doing such an experiment.

When we examined the effect of arterial taper on results, the convective and viscous terms in momentum equation were ignored. It should be noted that the taper influences both of these terms because it changes arterial area and blood velocity. Therefore, in analysing its real effect on results, these terms should be taken into consideration.

Another improvement in the model is changing the model used for peripheral beds so that it can take their reaction to blood flow reduction or increase into consideration.

In this study, the steady state momentum equation was used to approximate shear force at the artery wall. Other more accurate analytical solutions can be used to obtain this term like the Womersley solution [11].

In general, the developed numerical simulation is an excellent utility to examine the effect of parameters like

arterial stenosis and taper on the results, a task which was done in this study.

Conclusions

In this paper a computer simulation of blood flow was presented. Flow rate and pressure wave results for femoral artery were in good agreement with the published experimental results.

Power Law and Casson models were used for blood in addition to Newtonian one. The results of Casson model were more accurate than the Power Law model.

The simulation of stenosis showed that arterial stenosis produces pressure and flow reduction after it and a more severe stenosis produces more reduction.

The results showed that the effect of taper on pressure and flow waves depends on difference between areas of no tapered and tapered arteries. Tapering does only have a negligible effect on results.

Acknowledgements

The authors thank A. Dabiri for his technical assistance.

References

- [1] STERGIOPULOS N., YOUNG D.F. and ROGGE T.R. (1992): 'Computer Simulation of Arterial Flow with Applications to Arterial and Aortic Stenosis', *J. Biomechanics*, **25** (12), pp. 1477-1488.
- [2] RAINS J.K., JAFFRIN M.Y., and SHAPIRO A.H. (1974): 'A Computer Simulation of Arterial Dynamics in the Human Leg', *J. Biomechanics*, **7**, pp. 77-91.
- [3] PORENTA G., YOUNG D.F., ROGGE T.R. (1986): 'A Finite-Element Model of Blood Flow in Arteries Including Taper, Branches, and Obstructions', *J. Biomech. Engng*, **108**, pp. 161-167.
- [4] WAN J., STEELE B., SPICER S.A., STROHBAND S., FEIJOO G.R., HUGHES Th.J.R., and TAYLOR CH.A. (2002): 'A One-dimensional Finite Element Method for Simulation-Based Medical Planning for Cardiovascular Disease', *Computer Methods in Biomechanics and Biomedical Engineering*, **5** (3), pp. 195-206.
- [5] STREETER V.L., KEITZER W.F., and BOHR D.F. (1963): 'Pulsatile Pressure and Flow through Distensible Vessels', *Cir. Res.*, **13**, pp. 3-20.
- [6] JOHNSTON B.M., JOHNSTON P.R., CORNEY S., KILPATRICK D., (2004): 'Non-Newtonian Blood Flow in Human Right Coronary Arteries: Steady State Simulations', *J. Biomechanics*, **37**, pp. 709-720.
- [7] YOUNG D.F. and TSAI F.Y. (1973): 'Flow Characteristics in Models of Arterial Stenoses-II. Unsteady Flow', *J. Biomechanics*, **6**, pp. 547-559.
- [8] NICHOLS W.W. and O'ROUKE M.F. (1998): 'McDonald's blood flow in arteries, theoretical, experimental and clinical principles', (Oxford University Press, Inc., New York), pp. 170-200.
- [9] OLUFSEN M.S. (1999), 'Structured Tree Outflow Condition for Blood Flow in Large Systemic Arteries', *American Journal of Physiology*, **276**, pp. 257-268.
- [10] NICHOLS W.W. and O'ROUKE M.F. (1998): 'McDonald's blood flow in arteries, theoretical, experimental and clinical principles', (Oxford University Press, Inc., New York), pp. 91.
- [11] WOMERSLEY, J.R., (1957), 'An elastic tube theory of pulse transmission and oscillatory flow in mammalian arteries', WADC Tech. Rept. 56-64.